https://doi.org/10.1016/j.jmmm.2016.09.102

Magneto-caloric effect of $Fe_xZr_yB_{100-x-y}$ metallic ribbons for room temperature magnetic refrigeration

Guo D.Q.[1], Chan K.C.[1,*], Xia L.[2] and Yu P.[3]

1. Department of Industrial and Systems Engineering, Hong Kong Polytechnic University, Hung Hom, Hong Kong, China

2. Laboratory for Microstructure, Shanghai University, Shanghai 200072, China

3. College of Physics and Electronic Engineering, Chongqing Normal University, Chongqing 401331, China

*Corresponding author. E-mail address: kc.chan@polyu.edu.hk

Abstract

Among various amorphous magnetic materials, even though Fe-based materials do not have high magnetocaloric effect (MCE), their advantages of tunable Curie temperature (T_C) and low cost have attracted considerable attention in regard to room temperature magnetic refrigeration applications. With the aim of enhancing the MCE, the influence of boron addition on Fe-based amorphous materials was investigated in this study. $Fe_{94-x}Zr_6B_x$ (x=5, 6, 8 and 10), $Fe_{91-y}Zr_9B_y$ (y=3, 4, 5, 6, 8 and 10) and $Fe_{89-z}Zr_{11}B_z$ (z=3, 4, 5, 6, 8 and 10) specimens were made in ribbon form and their magnetocaloric effect was investigated. The Curie temperature (T_C) of all three series of ribbons underwent an almost linear increase, and the peak magnetic entropy change, $\left|\Delta S_M^{peak}\right|$ (obtained in a magnetic field of 1.5 T), generally increases with increasing

boron content. The results further show that the $Fe_{86}Zr_9B_5$ ribbon exhibits a relatively large $\left|\Delta S_M^{peak}\right|$ value of 1.13 J/kgK at 330 K and a large refrigerant capacity value of 135.6 J/kg under 1.5 T. On the basis of these results, although there is still much scope for improvement before totally replacing the conventional cooling method, the Fe-based amorphous ribbon can be seen as a promising magnetocaloric material for room temperature magnetic refrigeration applications.

Keywords: amorphous materials, magnetic materials, magnetocaloric effect.

1. Introduction

Twenty years after the first discovery in 1860 by William Thomson[1)] that the temperature of a magnetic material can be influenced by external magnetic fields, Warburg[2)] explained the magnetocaloric effect (MCE) in which the temperature of Fe increases upon magnetization and decreases upon demagnetization. However, MCE did not attract much attention until 1976 when Brown[3)] first realized that MCE could be applied for room temperature magnetic refrigeration (MR). Compared with conventional refrigeration, MR is more energy-saving and environmentally-friendly[4, 5)]. The coefficient of performance (COP) of MR can be as high as 15; however, the COPs in conventional refrigeration only range from 2 to 6[6)]. Differing from conventional refrigeration that uses ozone-depletion gas as the refrigerant, MRs

generally use liquid for cooling and solid magnetic materials as the refrigerants, with no harmful gas emission.

The most challenging aspect is to search for new materials with their MCE sufficiently large for the MR applications, since the MCE of the working materials is of great importance to the performance of the MR. To quantify the MCE, the working temperature range (ΔT), together with the peak magnetic entropy change (ΔS_M^{peak}), have been acknowledged as the two main parameters in determining the refrigerant capacity (RC)[7]. Materials exhibiting second order phase transition which display a ΔS_M^{peak} over a wide temperature range, are preferred, because these working materials need to be effective under different temperature conditions. Since Duwez[8] first synthesized Fe-based metallic glass in 1967, much attention has been paid to their superior properties[9-18]. These materials have lower cost than rare-earth based materials, excellent soft magnetic properties without hysteresis losses which make it possible to work in high frequencies with fast response, and tunable Curie temperatures (T_C) which can be easily realized by adjusting the composition[14]. Most of the Fe-based materials have Curie temperatures far above room temperature, which means that the MCE of these materials cannot reach their maximum values under the room temperature range, and are therefore not ideal for MR applications at room temperature. FeZrB metallic glasses, however, are better candidates because their T_C is closer to room temperature. In this work, the magnetocaloric effect of FeZrB metallic glasses was systematically studied.

2. Experimental details and data analysis

Ingots with nominal composition $Fe_{94-x}Zr_6B_x$ (x=5, 6, 8 and 10), $Fe_{91-y}Zr_9B_y$ (y=3, 4, 5, 6, 8 and 10) and $Fe_{89-z}Zr_{11}B_z$ (z=3, 4, 5, 6, 8 and 10) were melted repeatedly in a vacuum arc melter machine under an argon atmosphere. Ribbons of 0.02 mm in thickness and 1.5 mm width were obtained in a spinning copper roller machine with a single roller under an argon atmosphere. X-ray diffraction (XRD) investigations were performed using a Rigaku diffractometer with Cu-*Kα* radiation in order to confirm the amorphous state of the specimens. The soft magnetic properties of these ribbons were investigated by carrying out magnetic hysteresis tests. The measurement was performed on a Lakeshore 7407 vibrating sample magnetometer (VSM). The magnetic hysteresis loops were tested in conditions where the magnetic field decreased from 0.7 T to -0.7 T, and then increased back to 0.7 T, in 0.007 T steps. The hysteresis loops for each ribbon sample were tested both below and above its Curie temperature. The magnetization of the ribbons was also characterized on the VSM. The temperature range for the magnetization test was from 250 K to 400 K, in 10 K steps. At each temperature point, the magnetization curve of each ribbon was obtained under a field increasing from 0 to 1.5 T in 0.005 T steps. The MCE of the ribbons was characterized by calculating the working temperature range (ΔT) and the peak magnetic entropy change (ΔS_M^{peak}). According to one of the fundamental Maxwell's relations[19], the ΔS_M can be obtained as follows:

$$\left(\partial S(T,H)/\partial H\right)_T = \left(\partial M(T,H)/\partial T\right)_H \qquad (1)$$

where T represents for the temperature, H the magnetic field and M the magnetization. Integrating Eq. (1), under isothermal conditions, goes:

$$\Delta S(T,\Delta H)=\int_{H_1}^{H_2}(\partial M(T,H)/\partial T)_H\,dH\ . \qquad (2)$$

In a magnetic solid, the total entropy is contributed by three parts:

$$S(T,H)=S_M(T,H)+S_{Lat}(T)+S_{El}(T) \qquad (3)$$

where S_M represents for the magnetic entropy, S_{Lat} the lattice entropy and S_{El} the electronic entropy. In an isothermal process at a fixed temperature T,

$$\Delta S_M(T,\Delta H)=\Delta S(T,\Delta H)=\int_{H_1}^{H_2}(\partial M(T,H)/\partial T)_H\,dH \qquad (4)$$

To calculate the refrigerant capacity (RC), the following equation was used:

$$RC(\Delta H)=\int_{T_{cold}}^{T_{hot}}\left|\Delta S_M(T,\Delta H)\right|dT\ . \qquad (5)$$

To simplify the calculations and allow comparison with the results in the literature, RC can also be obtained by:

$$RC(\Delta H)=\left|\Delta S_M^{peak}\right|\times\delta T_{FWHM}. \qquad (6)$$

where δT_{FWHM} is the full width at the half maximum of ΔS_M.

3. Results and discussion

The ribbons of $Fe_{94-x}Zr_6B_x$ (x=5, 6, 8 and 10), $Fe_{91-y}Zr_9B_y$ (y=3, 4, 5, 6, 8 and 10) and $Fe_{89-z}Zr_{11}B_z$ (z=3, 4, 5, 6, 8 and 10) were successfully fabricated. The X-ray diffraction tests were carried out and the result of each specimen is presented in Fig. 1. Every one of the XRD patterns shows a broad wave pack around where $2\theta = 45°$ and no sharp crystalline peak. Based on these XRD results, all the specimens are considered to be amorphous.

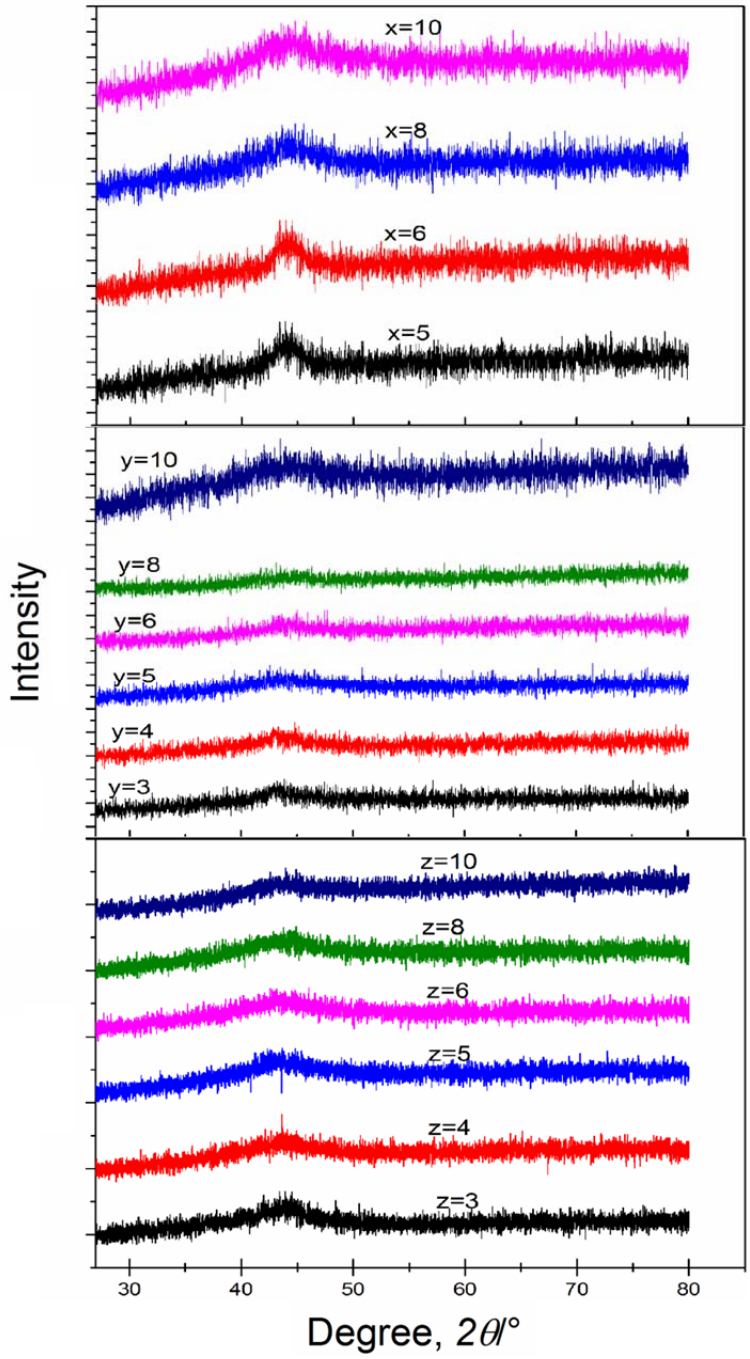

Figure 1. XRD results of $Fe_{94-x}Zr_6B_x$ (x=5, 6, 8 and 10), $Fe_{91-y}Zr_9B_y$ (y=3, 4, 5, 6, 8 and 10) and $Fe_{89-z}Zr_{11}B_z$ (z=3, 4, 5, 6, 8 and 10) ribbons

In order to calculate the MCE of the ribbons, magnetization curves were obtained over a wide temperature range. The magnetization curves in Fig. 2 are the results for three typical ribbons representing $Fe_{94-x}Zr_6B_x$ (x=5, 6, 8 and 10), $Fe_{91-y}Zr_9B_y$ (y=3, 4, 5, 6, 8 and 10) and $Fe_{89-z}Zr_{11}B_z$ (z=3, 4, 5, 6, 8 and 10), respectively. All three figures

show that the saturation magnetization increases as the temperature decreases. In addition, the temperature dependence of the magnetization curve shape indicates that

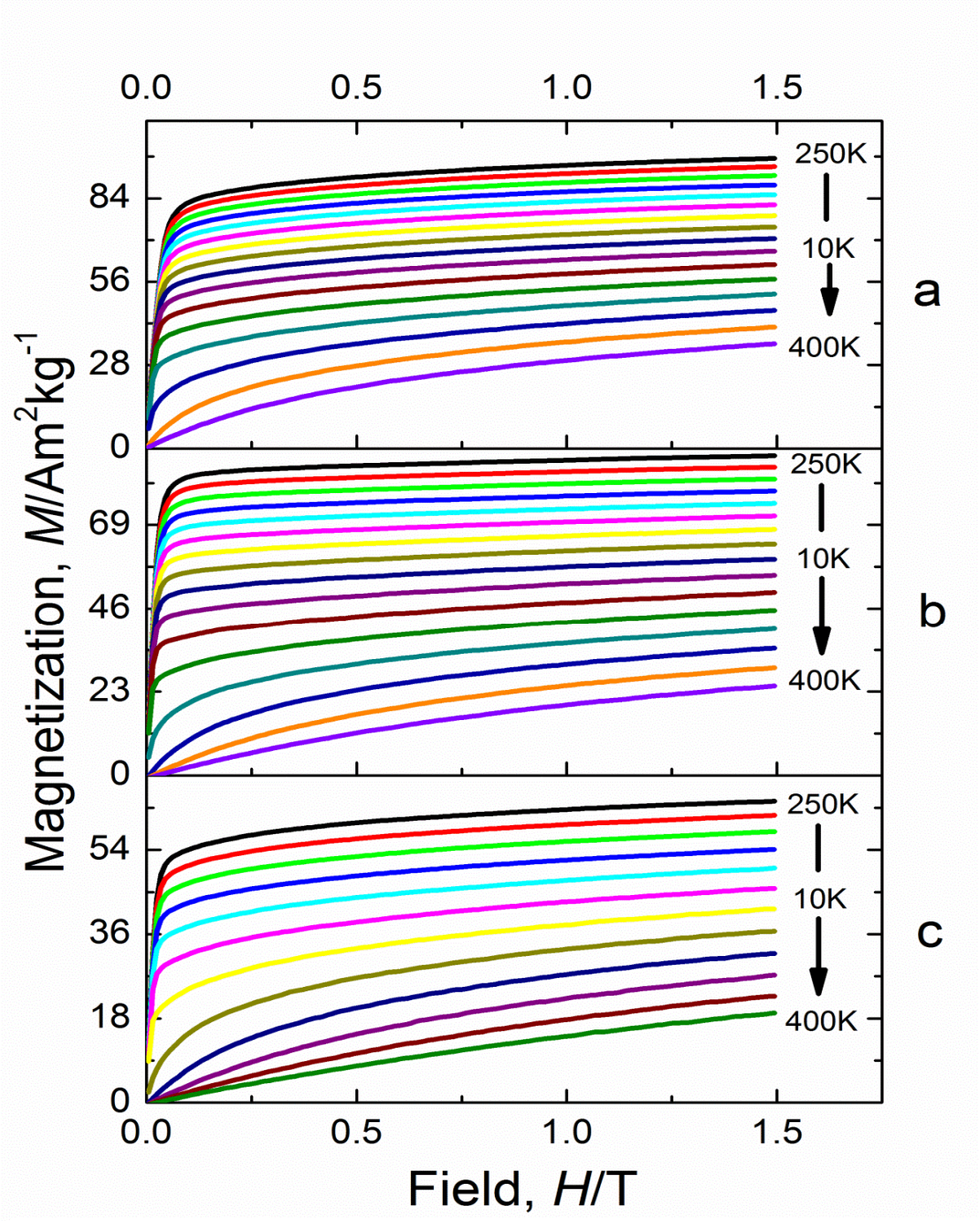

Figure 2. Magnetization curves of three representative samples (a) Fe86Zr6B8, (b) Fe83Zr9B8 and (c) Fe81Zr11B8.

all these ribbon samples undergo a second order magnetic transition (SOMT). The magnetic hysteresis loops are shown in Fig. 3. The magnetic hysteresis loops were

obtained under a magnetic field varying from -0.7 T to +0.7 T in steps of 0.007 T. All of the amorphous ribbons exhibited excellent soft magnetic properties since very

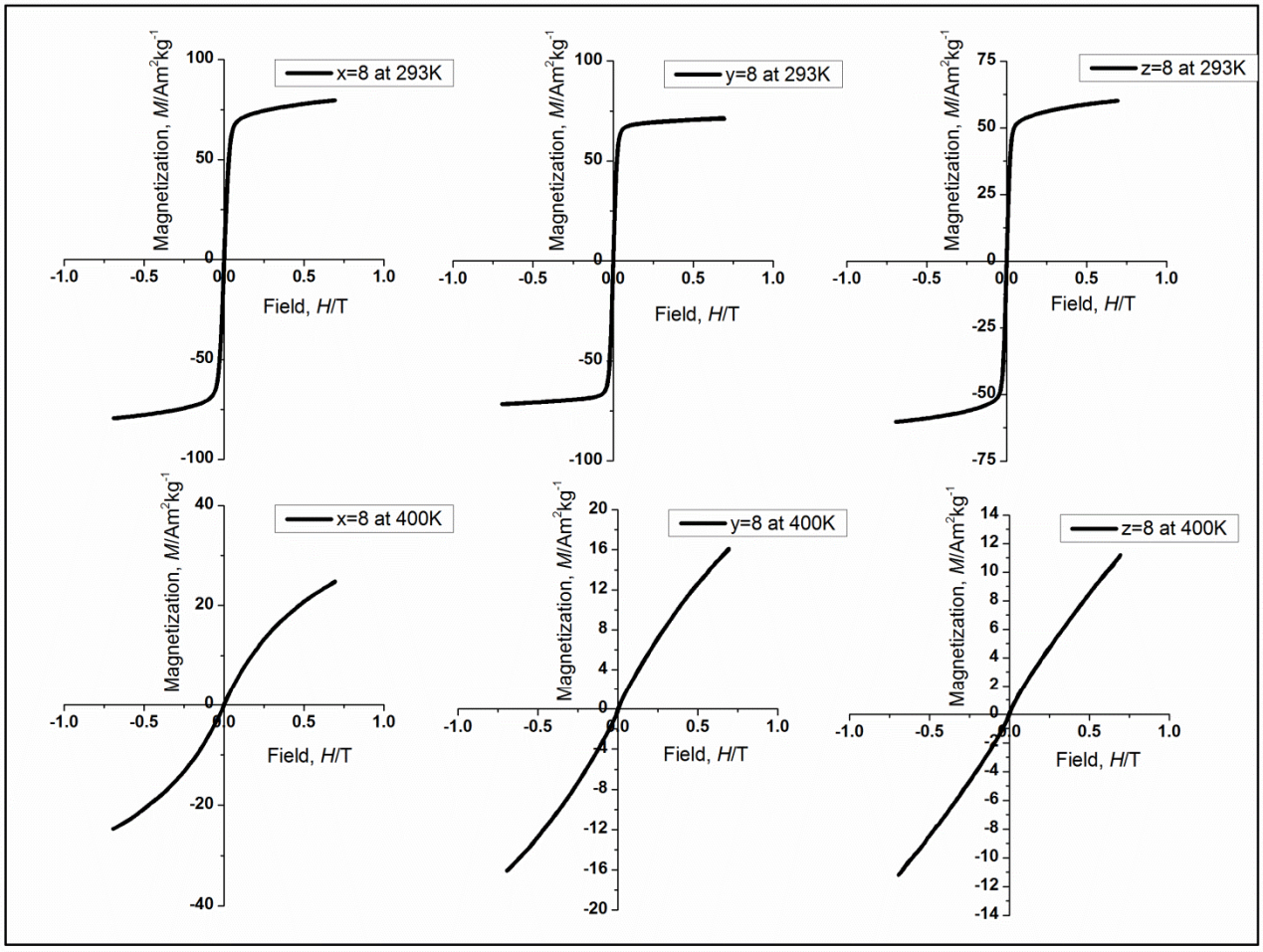

Figure 3. Hysteresis loops of samples (a) Fe86Zr6B8, (b) Fe83Zr9B8 and (c) Fe81Zr11B8 under different temperatures.

small hysteresis and nearly zero coercivity were found in each hysteresis loop. At the temperature of 400K, it was found that the hysteresis loops do not correspond to a paramagnetic system. It could be due to the presence of nanoparticles or clusters. They are commonly reported in Fe-based amorphous materials, but are too small to be identified by XRD tests [20-23]. Based on the results of the magnetization curves, the temperature dependence of $|\Delta S_M|$ was calculated according to Eq. (2) and the curves are shown in Fig. 4, with a maximum value corresponding to the largest entropy

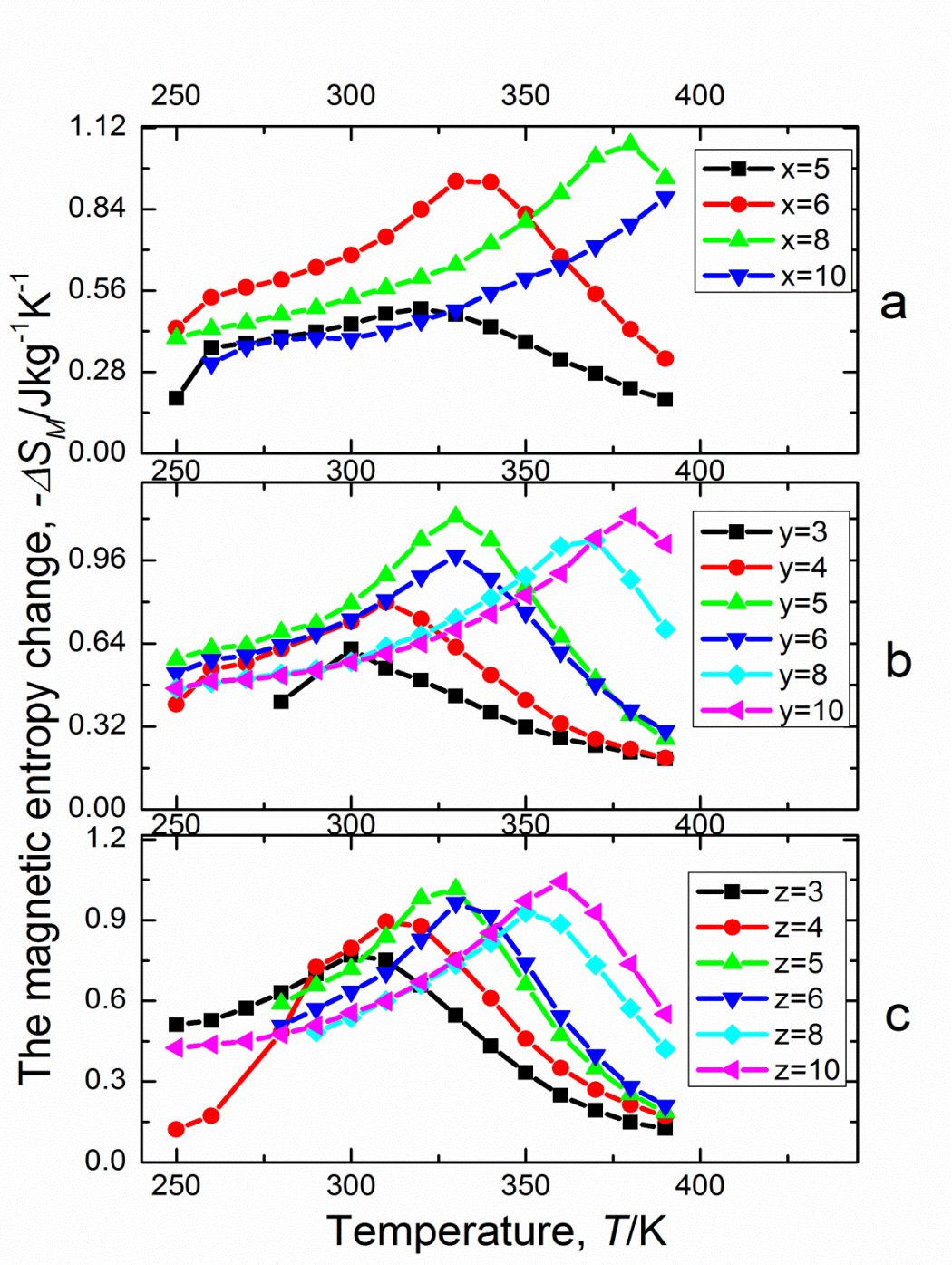

Figure 4. The magnetic entropy change vs. temperature curves of the ribbon samples (a) Fe86Zr6B8, (b) Fe83Zr9B8 and (c) Fe81Zr11B8.

change. The broad caret-like shape in each curve also illustrates that the specimens underwent a second order magnetic transition. On the basis of the curves in Fig. 3, the peak magnetic entropy change ($\left|\Delta S_M^{peak}\right|$) of each sample can be readily obtained. For comparison, the boron content dependence of the $\left|\Delta S_M^{peak}\right|$ curves are shown in Fig. 5a. In general, the $\left|\Delta S_M^{peak}\right|$ tends to increase as the content of boron increases in all

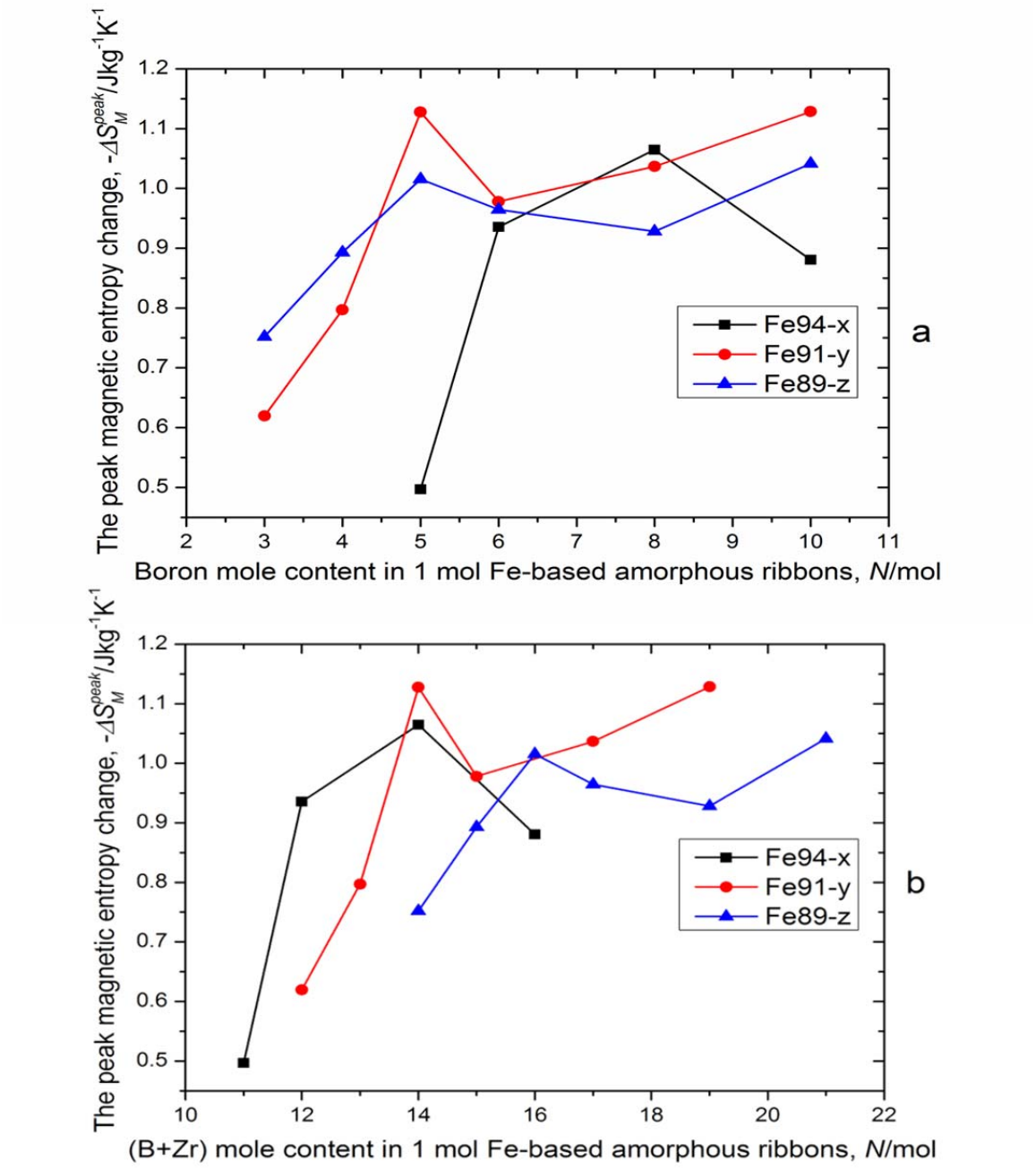

Figure 5. The peak magnetic entropy change vs. the (a) boron and (b) boron + zirconium mole content in 1 mol Fe-based amorphous ribbons curve.

of the three series of ribbons. Fig. 4b shows the (B + Zr) content dependence of the $\left|\Delta S_M^{peak}\right|$. To obtain the Curie temperature of each ribbon sample, their temperature-dependent magnetization values were measured in a fixed magnetic field of 0.0346 T with the temperature changing from 400 K to 250 K. For illustration purpose, Fig. 6 shows only three samples, each corresponding to one of the three

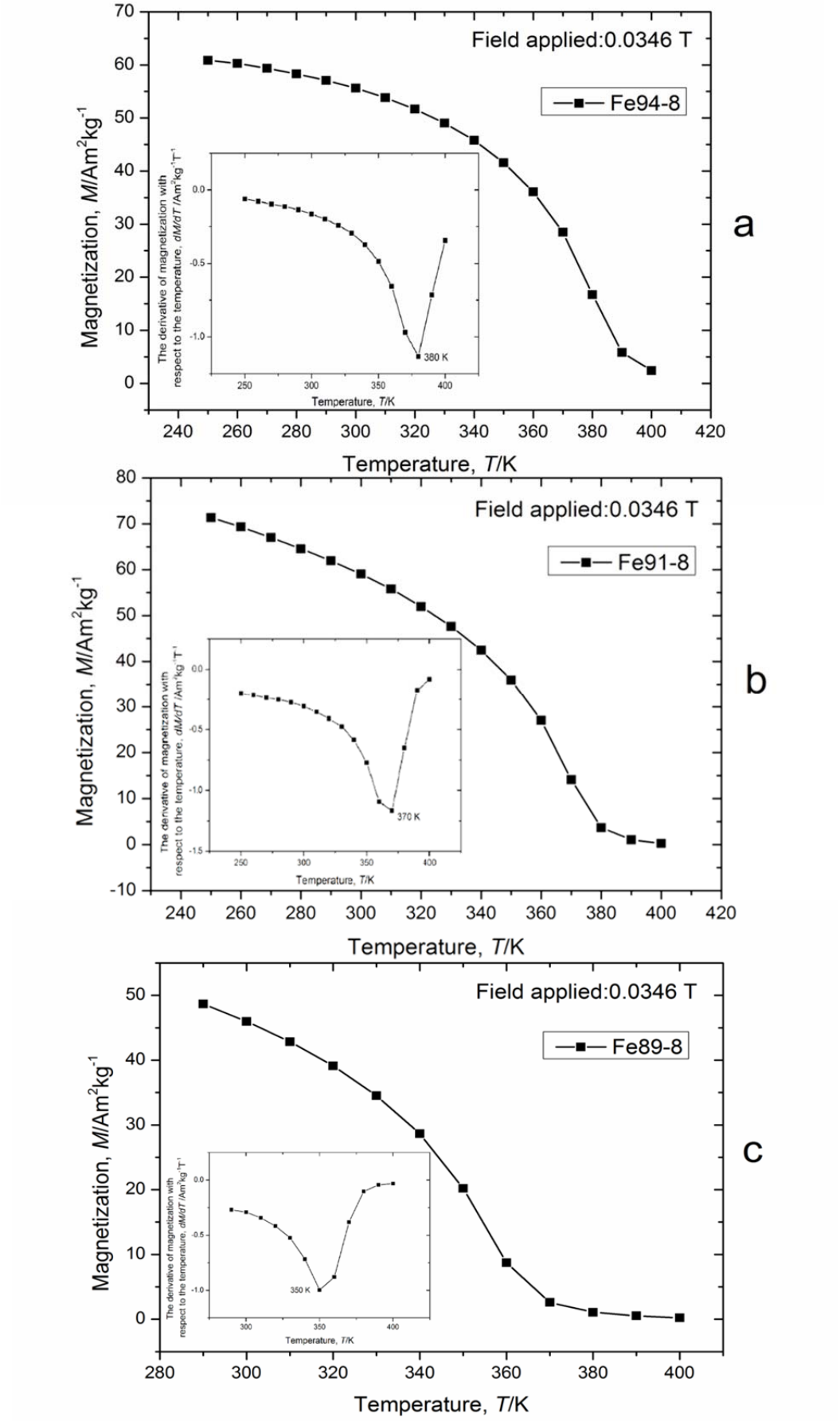

Figure 6. Temperature dependence of magnetization curves of (a) Fe86Zr6B8, (b) Fe83Zr9B8 and (c) Fe81Zr11B8 under the cooling process from 400 K to 250 K at a field of 0.0346 T.

series. The inset of each figure is the temperature dependence of the derivative of the magnetization with respect to the temperature (*dM/dT*) curve calculated from Fig. 6. The temperature where *dM/dT* reaches its minimum value in each inset corresponds to the Curie temperature. Similar to the $\left|\Delta S_M^{peak}\right|$, the boron content dependence of the T_C curves were plotted as solid lines with dots, in Fig. 7 for comparison. The dash lines are the results of the linear

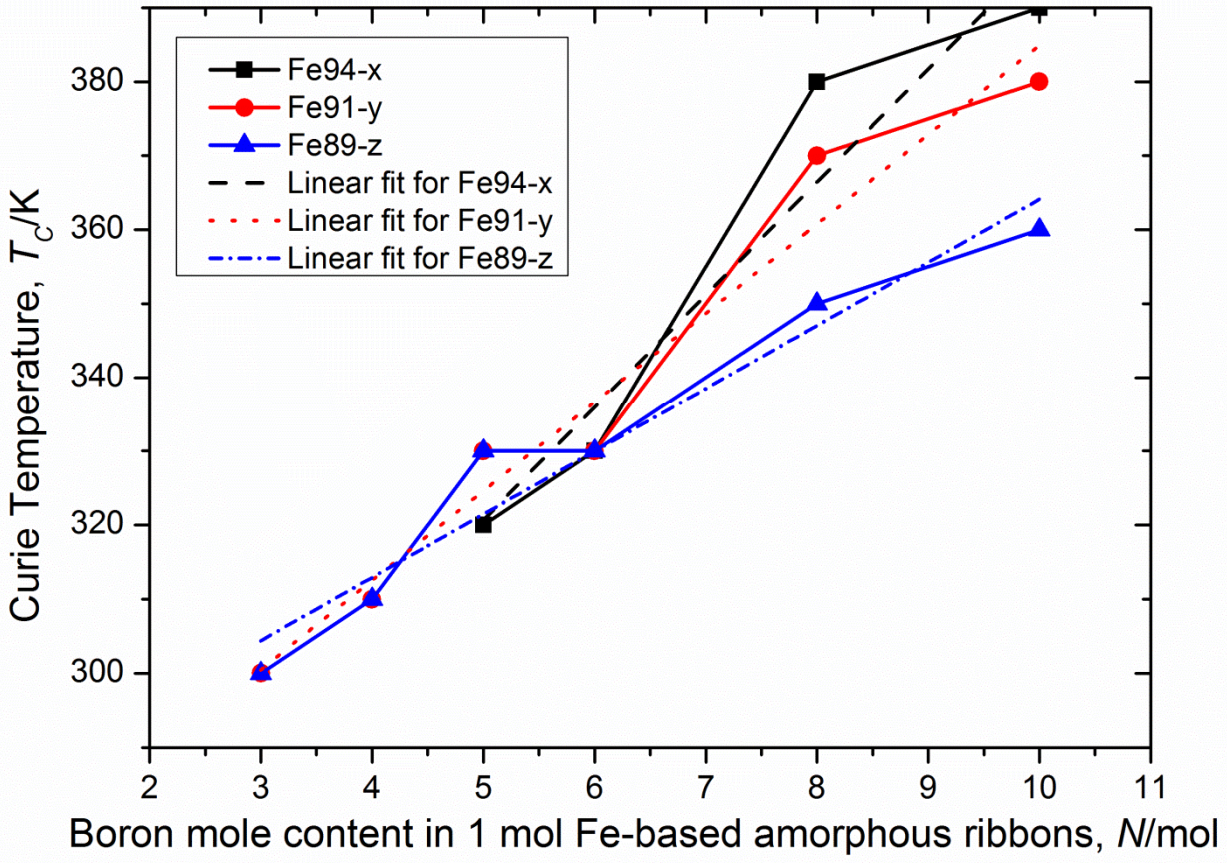

Figure 7. The Curie temperature vs. the boron mole content in 1 mol Fe-based amorphous ribbons curve.

regression. The fitting results for $Fe_{94-x}Zr_6B_x$, $Fe_{91-y}Zr_9B_y$ and $Fe_{89-z}Zr_{11}B_z$ are $T_C = [244 + 15 * (B) \pm 16]K$, $T_C = [264 + 12 * (B) \pm 10]K$ and $T_C = [278 + 8.5 * (B) \pm 4]K$, respectively, where B is the boron mole content in 1 mol

alloys. The change of the Curie temperature can be explained by a molecular field theory [24]:

$$T_C = J(r)Z_T S(S+1)/3k_B \qquad (7)$$

where *J(r)* represents for the distance-dependence of the inter-atomic exchange integral, Z_T, for the coordination about the T site, S is the atomic spin quantum number and k_B is Boltzmann's constant. With increasing addition of boron and a decreasing amount of iron, the distance between the Fe atoms increases, which leads to an increase of *J(r)*. Therefore, T_C increases on the basis of Eq. (7). On the other hand, with the substitution of boron for iron, the number of surrounding boron atoms for each iron atom site increases, which leads to an increase of Z_T. As a result, T_C also tends to increase on the basis of Eq. (7).

The refrigerant capacity of the amorphous ribbons can be calculated either from Eqs. (5) or (6). The difference between Eq. (5) and Eq. (6) is that the result of Eq. (5) is less and closer to the intrinsic magnetic property of the materials than that of Eq. (6). In order to better compare the results, however, the method used for calculating the RC in this work needs to be consistent with that in the literature. In this work, Eq. (6) was used for calculation. Comparing the magnetocaloric behavior of the present material with other FeZrB metallic ribbons[14], $\left|\Delta S_M^{peak}\right|$ of $Fe_{91}Zr_7B_2$ is found to be about 90% of that of the present material, $Fe_{86}Zr_9B_5$. Whereas, $\left|\Delta S_M^{peak}\right|$ of $Fe_{88}Zr_8B_4$ is only 78% of that of $Fe_{86}Zr_9B_5$ although T_C of the former (295 K) is slightly closer to the room temperature. When comparing with the magnetocaloric behavior of the $Fe_{92-x}Zr_7B_xCu_1$ amorphous ribbons studied before[21], the refrigerant capacities of the

present are higher. For those $Fe_{92-x}Zr_7B_xCu_1$ amorphous ribbons with Curie temperatures lower than 350 K, their refrigerant capacities are only less than 48 J/kg under 1.5 T. Whereas, the maximum RC value of the present material under the same condition can be almost three times as large as 48 J/kg. The magnetocaloric behavior, including the RC results of the as-spun amorphous ribbons, are summarized in Table 1, together with the results of some other Gd-based and Fe-based materials reported in the literature, for comparison.

Table 1. The magnetocaloric effect of the magnetic materials studied in this work and reported in the literature

Nominal composition	Structure	Magnetic Field (T)	T_C (K) from the experimental results	T_C (K) from the linear results	δT_{FWHM} (K)	$\left\|\Delta S_M^{peak}\right\|$ (J kg^{-1}K^{-1})	RC (J kg^{-1})	Ref.
$Fe_{89}Zr_6B_5$	Amorphous	1.5	320	319	110	0.50	55	This work
$Fe_{88}Zr_6B_6$	Amorphous	1.5	330	334	110	0.94	103	This work
$Fe_{86}Zr_6B_8$	Amorphous	1.5	380	364	110	1.06	116.6	This work
$Fe_{84}Zr_6B_{10}$	Amorphous	1.5	390	394	110	0.88	96.8	This work
$Fe_{88}Zr_9B_3$	Amorphous	1.5	300	300	80	0.62	49.6	This work
$Fe_{87}Zr_9B_4$	Amorphous	1.5	310	312	100	0.80	80	This work
$Fe_{86}Zr_9B_5$	Amorphous	1.5	330	324	120	1.13	135.6	This work
$Fe_{85}Zr_9B_6$	Amorphous	1.5	330	336	120	0.98	117.6	This work
$Fe_{83}Zr_9B_8$	Amorphous	1.5	370	360	120	1.04	124.8	This work
$Fe_{81}Zr_9B_{10}$	Amorphous	1.5	380	384	100	1.13	113	This work
$Fe_{86}Zr_{11}B_3$	Amorphous	1.5	300	303.5	100	0.77	77	This work

$Fe_{85}Zr_{11}B_4$	Amorphous	1.5	310	312	80	0.89	71.2	This work
$Fe_{84}Zr_{11}B_5$	Amorphous	1.5	330	320.5	90	1.02	91.8	This work
$Fe_{83}Zr_{11}B_6$	Amorphous	1.5	330	329	90	0.97	87.3	This work
$Fe_{81}Zr_{11}B_8$	Amorphous	1.5	350	346	110	0.93	102.3	This work
$Fe_{79}Zr_{11}B_{10}$	Amorphous	1.5	360	363	110	1.04	114.4	This work
$Fe_{91}Zr_7B_2$	Amorphous	1.5	250	N/A	N/A	1.04	N/A	14)
$Fe_{88}Zr_8B_4$	Amorphous	1.5	295	N/A	N/A	0.88	N/A	14)
$Fe_{92-x}Zr_7B_xCu_1(x<7)$	Amorphous	1.5	250~350	N/A	N/A	<1.35	<48	25)
$Fe_{92-x}Zr_7B_xCu_1(6<x<24)$	Amorphous	1.5	350~530	N/A	N/A	1.35~1.7	48~90	25)
$Fe_{80}Cr_4B_{10}Zr_5Gd_1$	Amorphous	1.5	360	N/A	120	0.91	110	26)
$Fe_{75}Nb_{10}B_{15}$	Amorphous	1.5	250	N/A	190	0.60	115	27)
$Fe_{79}Nb_7B_{14}$	Amorphous	1.5	372	N/A	N/A	1.07	N/A	28)
$(Fe_{70}Ni_{30})_{89}Zr_7B_4$	Amorphous	1.5	342	N/A	N/A	0.70	N/A	16)
$Fe_{64}Mn_{14}CoSi_{10}B_{11}$	Amorphous	1.5	457	N/A	N/A	0.83	N/A	29)
$Fe_{72}Ni_{28}$	Amorphous	1.5	333	N/A	149	0.49	73	30)
$(Fe_{85}Co_{15})_{75}Nb_{10}B_{15}$	Amorphous	1.5	440	N/A	124	0.82	102	31)
$Gd_{55}Al_5Fe_{40}$	Amorphous	5.0	222	N/A	197	2.7	532	32)
$Gd_{60}Fe_{20}Co_{10}Al_{10}$	Amorphous	5.0	222	N/A	167	4.4	736	33)
$Gd_5Si_2Ge_2$	Crystalline	5.0	276	N/A	16.5	18.5	305	34)

Clearly, the magnetocaloric effect has a lot to do with the maximum applied magnetic field. As a result, to make the comparison of the MCE between different materials

meaningful and accurate, the comparison should be carried out in the same condition. In such a case, the following relation:

$$\left|\Delta S_M(T,H)\right| \propto H^n , \qquad (8)$$

is applied[18, 35], where n is an exponent which is a reflection of the material's intrinsic property. According to Eq. (8), the value of n can be calculated by

$$n = d\ln\left|\Delta S_M\right| / d\ln H . \qquad (9)$$

The curves in Fig. 8 show the temperature dependence of the n value of the $Fe_{86}Zr_9B_5$

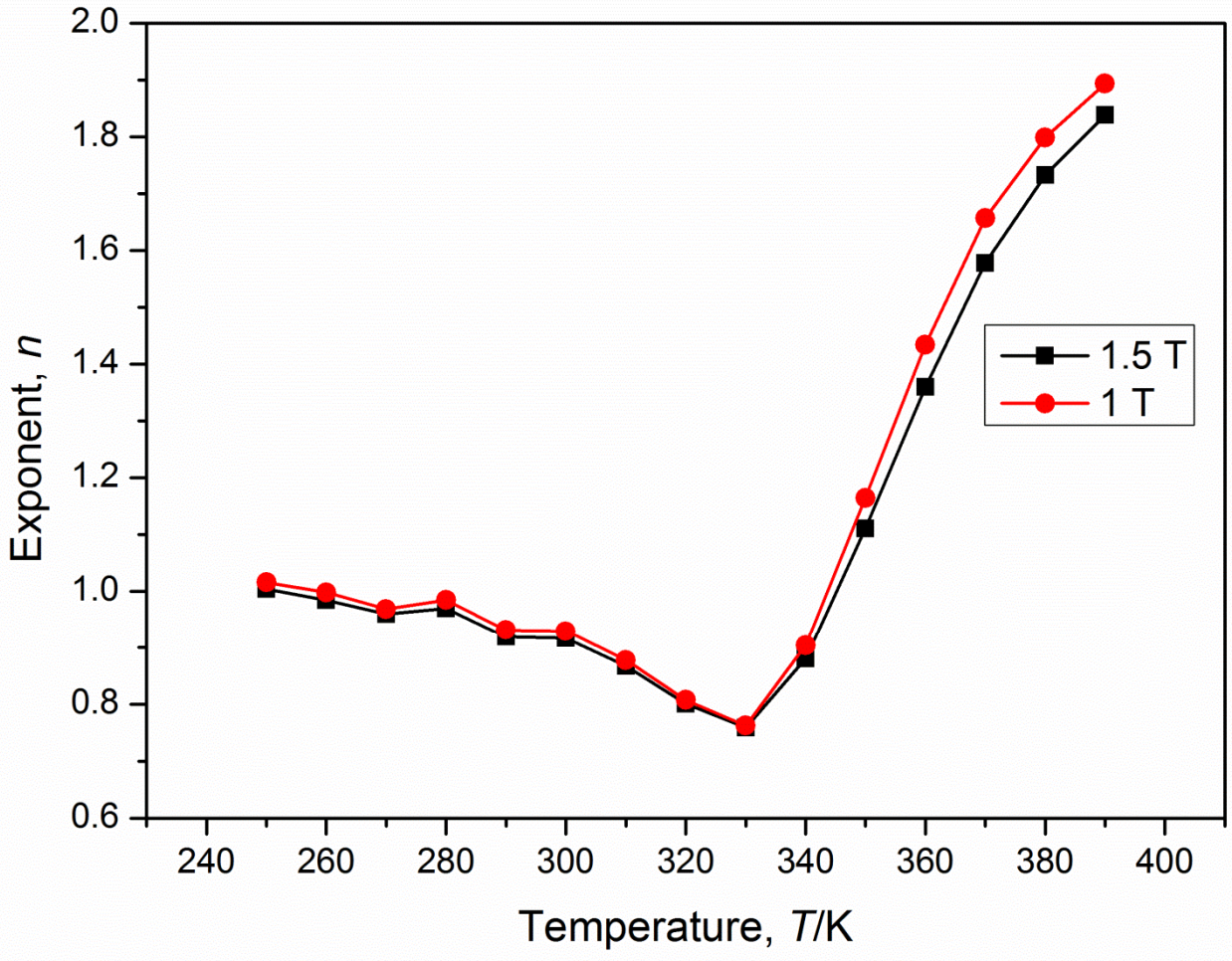

Figure 8. Temperature dependence of the exponent for ribbon sample Fe86Zr9B5 at two different maximum applied magnetic fields.

sample under magnetic fields of 1.0 T and 1.5 T respectively. It can be seen that the *n* value is about 0.75 at the Curie temperature (330 K). On the basis of the *n* value and Eq. (8), the magnetic entropy change of $Fe_{86}Zr_9B_5$ under different magnetic fields can be easily calculated. While the maximum field reaches 5 T, the peak magnetic entropy change of $Fe_{86}Zr_9B_5$ increases to 2.76 J/kgK which is larger than those of $Fe_{77}Gd_3Cr_8B_{12}$ (2.31 J/kgK) and $Fe_{75}Gd_5Cr_8B_{12}$ (2.34 J/kgK) under 5 T[36]. Based on this $\left|\Delta S_M^{peak}\right|$ value, the RC of $Fe_{86}Zr_9B_5$ becomes 331 J/kg on the assumption that δT_{FWHM} remains the same as that under 1.5 T. The reality is, however, with the increase of the maximum applied magnetic field, δT_{FWHM} will be larger. According to the result of Franco[37], the field dependence of RC value can be summarized as:

$$RC \propto H^{1+1/\delta}. \qquad (10)$$

where δ can be obtained from the field dependence of the magnetization at the Curie temperature[37]:

$$M \propto H^{1/\delta}. \qquad (11)$$

On the basis of the magnetization curves of the $Fe_{86}Zr_9B_5$ amorphous ribbon, the value of δ can be obtained by fitting the M-H curve. And the fitting result is:

$$M = 44.1298 \times H^{0.2101}, \qquad (12)$$

where the δ value is 4.760. According to Eq.(10), RC value of $Fe_{86}Zr_9B_5$ is therefore obtained to be 582.10 J/kg when $H_{\max}$ changes from 1.5 T to 5 T. The result makes sense since $Gd_5Si_2Ge_2$, a well-known magnetic material, exhibits a RC value of just 305 J/kg under 5 T, which is only about half value of that of $Fe_{86}Zr_9B_5$, as listed in Table 1[34]. In general, the $\left|\Delta S_M^{peak}\right|$ of the Fe-based magnetic materials is

smaller than that of Gd-based magnetic materials, as can be seen in Table 1, however, the rather lower fabrication cost of Fe-based materials than that of Gd-based ones plays an important role in industrialization. In addition, due to the compensation of the large δT_{FWHM}, the RC values of the Fe-based and the Gd-based magnetic materials are comparable. In addition, with the Curie temperatures being closer to room temperature, the Fe-based materials have more potential for room temperature applications.

4. Conclusions

In this study, three new Fe-based series of glassy ribbons were designed and successfully fabricated. The magnetocaloric effect of those Fe-based amorphous ribbons was extensively studied. The results indicate that small replacement of boron with iron could obviously change both the Curie temperature and the peak magnetic entropy change. With increasing the amount of boron, all specimens in the three series of ribbons tend to exhibit larger peak magnetic entropy changes as well as Curie temperatures. In order to apply this kind of material into room temperature refrigeration, not only the peak magnetic entropy change and the refrigerant capacity but also the Curie temperature should be taken into consideration. In this work, $Fe_{86}Zr_9B_5$ exhibits a $\left|\Delta S_M^{peak}\right|$ value of 1.13 J/kgK at 330 K and a RC value of 135.6 J/kg. Although its $\left|\Delta S_M^{peak}\right|$ is not the largest among all the specimens, it is the most appropriate candidate for room temperature applications due to the fact that both its

$\left|\Delta S_M^{peak}\right|$ and RC are relatively larger than those of other materials with its T_C is relatively closer to room temperature.

Acknowledgement

This research was fully funded by the Research Committee of the Hong Kong Polytechnic University under research student project account code RT4T.

References

1) W. Thomson, II. On the thermoelastic, thermomagnetic, and pyroelectric properties of matter, Philosophical Magazine Series 5, **5** (1878) 4-27.
2) E. Warburg, Magnetische Untersuchungen, Ann. Phys-berlin., **249** (1881) 141-164.
3) G. V. Brown, Magnetic heat pumping near room temperature, J. Appl. Phys., **47** (1976) 3673-3680.
4) K. Gschneidner Jr and V. Pecharsky, Magnetocaloric materials, Annu. Rev. Mater. Sci., **30** (2000) 387-429.
5) K. A. GschneidnerJr, V. K. Pecharsky and A. O. Tsokol, Recent developments in magnetocaloric materials, Rep. Prog. Phys., **68** (2005) 1479-1539.
6) K. A. Gschneidner and V. K. Pecharsky, Magnetic refrigeration materials (invited), J. Appl. Phys., **85** (1999) 5365.
7) M. E. Wood and W. H. Potter, General analysis of magnetic refrigeration and its optimization using a new concept: maximization of refrigerant capacity, Cryogenics, **25** (1985) 667-683.
8) P. Duwez, Amorphous Ferromagnetic Phase in Iron-Carbon-Phosphorus Alloys, J. Appl. Phys., **38** (1967) 4096.

9) I. Skorvanek and J. Kovac, Magnetocaloric behaviour in amorphous and nanocrystalline FeNbB soft magnetic alloys, Czech. J. Phys., **54** (2004) D189-D192.

10) F. Johnson and R. D. Shull, Amorphous-FeCoCrZrB ferromagnets for use as high-temperature magnetic refrigerants, J. Appl. Phys., **99** (2006) 08K909.

11) V. Franco, A. Conde and L. F. Kiss, Magnetocaloric response of FeCrB amorphous alloys: Predicting the magnetic entropy change from the Arrott–Noakes equation of state, J. Appl. Phys., **104** (2008) 033903.

12) Y. K. Fang, C. C. Yeh, C. C. Hsieh, C. W. Chang, H. W. Chang, W. C. Chang, X. M. Li and W. Li, Magnetocaloric effect in Fe–Zr–B–M (M=Mn, Cr, and Co) amorphous systems, J. Appl. Phys., **105** (2009) 07A910.

13) A. Makino, T. Kubota, C. Chang, M. Makabe and A. Inoue, FeSiBP Bulk Metallic Glasses with Unusual Combination of High Magnetization and High Glass-Forming Ability, Mater. Trans., **48** (2007) 3024-3027.

14) P. Álvarez, J. S. Marcos, P. Gorria, L. F. Barquín and J. A. Blanco, Magneto-caloric effect in FeZrB amorphous alloys near room temperature, J. Alloy. Compd., **504** (2010) S150-S154.

15) J. Y. Law, V. Franco and R. V. Ramanujan, Influence of La and Ce additions on the magnetocaloric effect of Fe–B–Cr-based amorphous alloys, Appl. Phys. Lett., **98** (2011) 192503.

16) J. J. Ipus, H. Ucar and M. E. McHenry, Near Room Temperature Magnetocaloric Response of an (FeNi)ZrB Alloy, IEEE Trans. on Magn., **47** (2011) 2494-2497.

17) A. Waske, B. Schwarz, N. Mattern and J. Eckert, Magnetocaloric (Fe–B)-based amorphous alloys, J. Magn. Magn. Mater., **329** (2013) 101-104.

18) R. Caballero-Flores, V. Franco, A. Conde, K. E. Knipling and M. A. Willard, Influence of Co and Ni addition on the magnetocaloric effect in $Fe_{88-2x}Co_xNi_xZr_7B_4Cu_1$ soft magnetic amorphous alloys, Appl. Phys. Lett., **96** (2010) 182506-182503.

19) V. K. Pecharsky and K. A. Gschneidner, Magnetocaloric effect and magnetic refrigeration, J. Magn. Magn. Mater., **200** (1999) 44-56.

20) S.X. Zhou, B.S. Dong, J.Y. Qin, D.R. Li, S.P. Pan, X.F. Bian and Z.B. Li, The relationship between the stability of glass-forming Fe-based liquid alloys and the metalloid-centered clusters, J. Appl. Phys., **112** (2012) 023514.

21) Q. Yu, X.D. Wang, H.B. Lou, Q.P. Cao and J.Z. Jiang, Atomic packing in Fe-based metallic glasses, Acta Mater., **102** (2016) 116-124.

22) N. Lupu and H. Chiriac, Low Field Magnetic Properties of $Nd_{50}Fe_{40}Si_{10-x}Al_x$ Melt-Spun and Bulk Amorphous Alloys, Mater. Trans., **42** (2001) 670-673.

23) M. Aykol, A.O. Mekhrabov and M.V. Akdeniz, Nano-scale phase separation in amorphous Fe–B alloys: Atomic and cluster ordering, Acta Mater., **57** (2009) 171-181.

24) R. C. O'Handley, Physics of ferromagnetic amorphous alloys, J. Appl. Phys., **62** (1987) R15.

25) L.F. Kiss, T. Kemény, V. Franco and A. Conde, Enhancement of magnetocaloric effect in B-rich FeZrBCu amorphous alloys, J. Alloy Compd., **622** (2015) 756

26) D.Q. Guo, K. C. Chan and L. Xia, Influence of Minor Addition of Cr on the Magnetocaloric Effect in Fe-Based Metallic Ribbons, Mater. Trans., **57** (2016) 9-14.

27) J. J. Ipus, J. S. Blazquez, V. Franco, A. Conde and L. F. Kiss, Magnetocaloric response of $Fe_{75}Nb_{10}B_{15}$ powders partially amorphized by ball milling, J. Appl. Phys., **105** (2009) 123922-123926.

28) S.-G. Min, K.-S. Kim, S.-C. Yu and K.-W. Lee, The magnetization behavior and magnetocaloric effect in amorphous Fe–Nb–B ribbons, Materials Science and Engineering: A, **449-451** (2007) 423-425.

29) J. H. Lee, S. J. Lee, W. B. Han, H. H. An and C. S. Yoon, Magnetocaloric effect of $Fe_{64}Mn_{15-x}Co_xSi_{10}B_{11}$ amorphous alloys, J. Alloy. Compd., **509** (2011) 7764-7767.

30) H. Ucar, J. J. Ipus, V. Franco, M. E. McHenry and D. E. Laughlin, Overview of Amorphous and Nanocrystalline Magnetocaloric Materials Operating Near Room Temperature, Jom, **64** (2012) 782-788.

31) J. J. Ipus, J. S. Blázquez, V. Franco and A. Conde, Influence of Co addition on the magnetic properties and magnetocaloric effect of Nanoperm $(Fe_{1-X}Co_X)_{75}Nb_{10}B_{15}$ type alloys prepared by mechanical alloying, J. Alloy. Compd., **496** (2010) 7-12.

32) Q. Dong, B. Shen, J. Chen, J. Shen, F. Wang, H. Zhang and J. Sun, Large magnetic refrigerant capacity in $Gd_{71}Fe_3Al_{26}$ and $Gd_{65}Fe_{20}Al_{15}$ amorphous alloys, J. Appl. Phys., **105** (2009) 053908-053908-053904.

33) B. Schwarz, B. Podmilsak, N. Mattern and J. Eckert, Magnetocaloric effect in Gd-based $Gd_{60}Fe_xCo_{30-x}Al_{10}$ metallic glasses, J. Magn. Magn. Mater., **322** (2010) 2298-2303.

34) V. K. Pecharsky and J. K. A. Gschneidner, Giant Magnetocaloric Effect in $Gd_5(Si_2Ge_2)$, Phys. Rev. Lett., **78** (1997) 4494-4497.

35) V. Franco, A. Conde, J. M. Romero-Enrique and J. S. Blázquez, A universal curve for the magnetocaloric effect: an analysis based on scaling relations, J. Phys.: Condensed Matter, **20** (2008) 285207.

36) J. Law, R. Ramanujan and V. Franco, Tunable Curie temperatures in Gd alloyed Fe-B-Cr magnetocaloric materials, J. Alloy. Compd., **508** (2010) 14-19.

37) V. Franco and A. Conde, Scaling laws for the magnetocaloric effect in second order phase transitions: From physics to applications for the characterization of materials, Int. J. Refrigeration, **33** (2010) 465

Highlights:

- The magneto-caloric effect of FeZrB has been systematically studied.
- The $Fe_{86}Zr_9B_5$ ribbons exhibit an excellent magneto-caloric effect as compared to the well-known $Gd_5Si_2Ge_2$ and other reported FeZrB materials such as $Fe_{91}Zr_7B_2$ and $Fe_{92-x}Zr_7B_xCu_1$.
- This work gives more insight into the magnetocaloric effect of FeZrB amorphous ribbons.